JACS
JOURNAL OF THE AMERICAN CHEMICAL SOCIETY

COMMUNICATION

pubs.acs.org/JACS

Gated Channels in a Honeycomb-like Zinc−Dicarboxylate−Bipyridine Framework with Flexible Alkyl Ether Side Chains

Sebastian Henke and Roland A. Fischer*

Anorganische Chemie II, Organometallics & Materials, Ruhr-Universität Bochum, D-44780 Bochum, Germany

Supporting Information

ABSTRACT: Covalent functionalization of 1,4-benzenedicarboxylate (bdc) with methoxyethoxy groups induces conformational freedom in this molecule. Applying these 2,5-disubstituted bdc derivatives in metal−organic framework synthesis together with 4,4′-bipyridine as coligand yields novel honeycomb-like structures. The cylindrical channels of these materials are populated with flexible groups, which act as molecular gates for guest molecules. This allows highly selective sorption of CO_2 over N_2 and CH_4.

Metal−organic frameworks (MOFs) represent a young, rapidly developing class of porous materials. Due to their high pore volumes and exceptional specific surface areas, they are very interesting for a variety of applications, like gas storage,[1] catalysis,[2] or gas separation.[3] MOFs are hybrid materials constructed from cationic metal ions or metal−oxo clusters and anionic linkers. Yaghi and co-workers have demonstrated that the intrinsic features of the linkers play an important role for the topology of the network structure.[4] In particular, additional substituents at the carboxylate linkers may introduce control over alternative topologies.[4b] Therefore, the design of particular linkers in combination with the other MOF building blocks represents a tool for deriving novel MOFs with unusual structures.

Many isoreticular MOFs of the type $[M_2L_2P]_n$ (M = Zn^{2+}, Cu^{2+}; L = linear dicarboxylate linker; P = neutral pillar, e.g., 1,4-diazabicylco[2.2.2]octane, pyrazine, or 4,4′-bipyridine) are known.[5,6] All these MOFs are constructed from 2D layers of $[M_2L_2]_n$, interconnected in the third dimension by the pillar P. The 2D layers are most often square grids, but polymorphs with Kagome-type layers were reported recently for some zinc derivatives.[6] A dimeric paddlewheel building unit represents the characteristic inorganic brick of all known $[M_2L_2P]_n$ frameworks. Typically, the M^{2+} ions are five-fold coordinated in a square planar fashion by four carboxylate oxygen atoms of L and one axial nitrogen donor atom of P.

Herein we report the discovery of a framework of the composition $[Zn_2L_2P]_n$ (**1**) [L = 2,5-bis(2-methoxyethoxy)-1,4-benzenedicarboxylate (BME-bdc); P = 4,4′-bipyridine (bipy)], which exhibits a honeycomb-like topology that is unknown for MOFs of the $[M_2L_2P]_n$ family (Figures 1 and 2). The linker BME-bdc features flexible alkyl ether groups attached to the rigid phenyl ring, but the particular 2,5-disubstitution increases the conformational freedom of the carboxylate groups, which are tilted away from the plane of the phenyl ring. This favors the formation of a MOF structure with a rod-like structural motif instead of the otherwise preferred paddlewheel structural motif of the $[M_2L_2P]_n$ family.

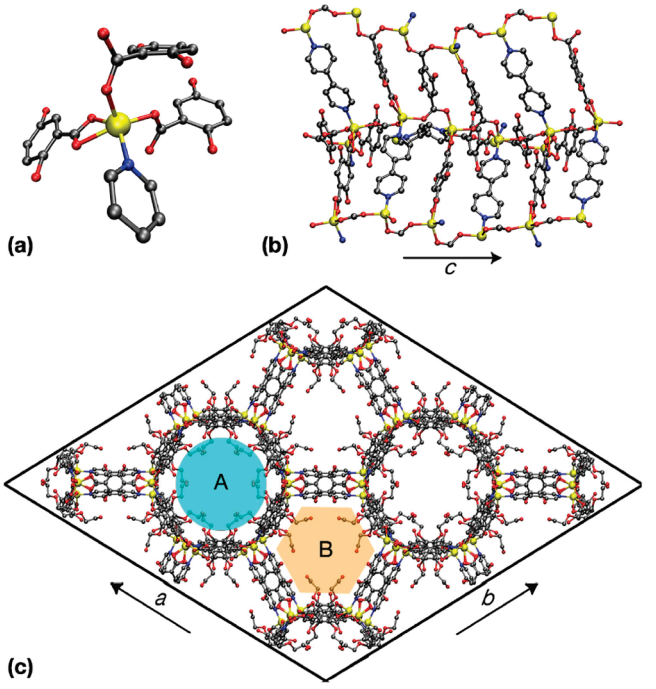

Figure 1. Structure of compound $\mathbf{1}_{as}$ as determined by single-crystal X-ray diffraction. (a) Zinc-centered inorganic building unit, (b) side view along the *c*-axis, and (c) unit cell in the [001] direction. The disordered $CH_3-O-C_2H_4$ chains of the BME-bdc linker are not shown in panels a and b; see Figure 2 for a schematic drawing. Zn, O, N, and C atoms are shown in yellow, red, blue, and gray, respectively. Hydrogen atoms were omitted for the sake of clarity. In panel c, channel types A and B are marked in cyan and beige.

H_2BME-bdc, bipy, and $Zn(NO_3)_2 \cdot 6H_2O$ were dissolved in a DMF/EtOH mixture and heated to 85 °C. After 48 h, colorless prismatic crystals of the composition $\{[Zn_2(BME\text{-}bdc)_2(bipy)]_n(DMF)_{2.3}(EtOH)_{0.4}\}$ were isolated in good yield ($\mathbf{1}_{as}$). The amount of solvent guests in the pores of the as synthesized material was calculated from thermogravimetric analysis (TGA) and elemental analysis data. The TGA of $\mathbf{1}_{as}$

Received: October 15, 2010
Published: January 28, 2011

dx.doi.org/10.1021/ja109317e | *J. Am. Chem. Soc.* 2011, 133, 2064–2067

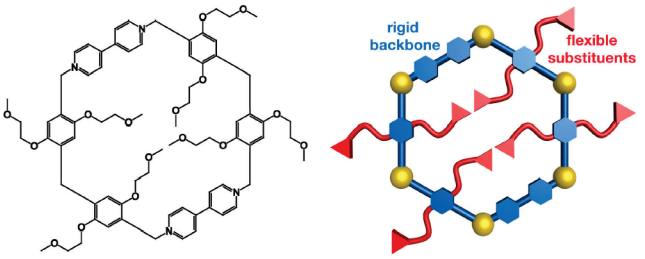

Figure 2. Sketch of the pore aperture of compound **1**. The rigid backbone of the framework is shown in blue, and the flexible alkyl ether substituents are shown in red.

shows a weight loss of 16.5% up to 150 °C. This amount fits well to the reported molecular composition (Figure S8).

Phase purity of $\mathbf{1}_{as}$ is demonstrated by comparison of the calculated powder X-ray diffraction (PXRD) pattern from the single-crystal data with the experimental one (Figure S3). Compound $\mathbf{1}_{as}$ crystallizes in the trigonal space group $R\bar{3}c$ (Table S1). As expected, not all atoms of the flexible substituent chains could be located in the single-crystal structure refinement due to the high disorder. Nevertheless, solid-state ^{13}C-MAS NMR and elemental analysis, as well as ^{1}H and ^{13}C NMR in DCl/D_2O/DMSO-d_6, of activated, solvent-free $\mathbf{1}_{dry}$ clearly support the reported composition (Figures S6 and S7).

The structure of $\mathbf{1}_{as}$ reveals isolated quasi-tetrahedrally coordinated Zn atoms, which are coordinated by one bipy ligand, one bidentate chelating carboxylate group, and two carboxylate groups, which bridge in *syn*−*anti* fashion to the next zinc center (Figure 1a). This unit is well known in inorganic coordination chemistry,[7] but, to the best of our knowledge, it has never been implemented in a robust, three-dimensional MOF structure before. The persistence of two different types of carboxylate groups (bridging and chelating) in the case of the activated (dried) material $\mathbf{1}_{dry}$ is evidenced by solid-state ^{13}C-MAS NMR and IR spectroscopy (Figures S6 and S14). An infinite chain of Zn atoms bridged by carboxylate groups runs along the *c*-axis of the structure of $\mathbf{1}_{as}$ (Figure 1b). Bipy and BME-bdc cross-link the zinc−carboxylate chains. This results in a three-dimensional structure with two different kinds of one-dimensional channels (Figure 1c). Essentially, the function of bipy in $\mathbf{1}_{as}$ is not that of a pillar between zinc−carboxylate sheets but rather an additional connector between infinite zinc−carboxylate rods.

The flexible $CH_3-O-C_2H_4$ chains of the BME-bdc linkers point into the channels. In fact, **1** represents a rigid MOF constructed from a honeycomb-like backbone structure and has solvent-like properties from the flexible groups, which lead to a polar, weakly Lewis basic environment within the pores (Figure 2). One prerequisite for the preference of the obtained honeycomb topology instead of the trivial tetragonal topology may be the increased conformational freedom of the carboxylate groups of the BME-bdc linker as compared to conventional bdc. Due to the steric repulsion induced by 2,5-disubstitution, coplanarity of the phenyl ring with the carboxylate groups caused by π-overlap is no longer preferred.

Three distinct conformations for the BME-bdc linker are found in $\mathbf{1}_{as}$ (Figure 3). The majority of the linkers exhibit the conformation shown in Figure 3b, where the carboxylate groups are twisted about 90° relative to each other. Such a conformation of the dicarboxylate linker is not possible in bdc, and thus $[Zn_2(bdc)_2(bipy)]_n$ cannot form the isoreticular framework of

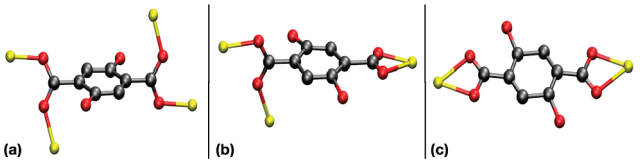

Figure 3. Depiction of the three different conformations of BME-bdc in the crystal structure of $\mathbf{1}_{as}$: 25% of the dicarboxylates in $\mathbf{1}_{as}$ are of type (a), 50% of type (b) and 25% of type (c). Hydrogen atoms and disordered $CH_3-O-C_2H_4$ groups are not shown. Zn, O, and C atoms are shown in yellow, red, and gray, respectively.

1; it rather forms an interpenetrated, pillared paddlewheel structure. Increased conformational freedom may also reduce the coordinative strain on the Zn^{2+} ions. In paddlewheel structures, Zn is forced into the square-pyramidal coordination geometry, whereas in **1**, Zn exhibits its typical quasi-tetrahedral coordination geometry with less steric crowding. This conformational freedom of BME-bdc is the key to form a different structure. In addition, the dipolar interactions of the flexible linkers within the channels may play a significant role as well. Furthermore, and very importantly, the steric features, in particular the lengths of the anionic linker L (BME-bdc) and the neutral connector P (bipy), must be similar in order to construct a framework of the topology of **1** (Figure S2). This is nicely evinced from the crystal structure of $[Zn_2(BME\text{-}bdc)_2(dabco)]_n$ (dabco = 1,4-diazabicyclo[2.2.2]octane). Dabco is another pillar P, which is very often utilized in $[M_2L_2P]_n$ systems. It is significantly shorter than bipy and BME-bdc. Therefore, $[Zn_2(BME\text{-}bdc)_2(dabco)]_n$ cannot form a honeycomb-like structure analogous to $[Zn_2(BME\text{-}bdc)_2(bipy)]_n$ and, in fact, crystallizes in the conventional pillared paddlewheel structure.[8]

Interestingly, the use of 2-(2-methoxyethoxy)benzenedicarboxylic acid (H_2ME-bdc), the monosubstituted analogue of H_2BME-bdc, leads to the (expected) interpenetrated pillared paddlewheel framework $\{[Zn_2(ME\text{-}bdc)_2(bipy)]_n(DMF)_x(EtOH)_y\}$ (**2**). Compound **2** has the same network topology and internal connectivity as $[Zn_2(bdc)_2(bipy)]_n$, also known as MOF-508 (Figure S9, Table S2).[5b−5d] This comparison nicely shows the importance of 2,5-disubstitution at the bdc linker to trigger the formation of the unique topology of **1**. Accordingly, we synthesized two related 2,5-substituted H_2bdc derivatives, 2,5-bis(3-methoxypropoxy)benzenedicarboxylic acid (H_2BMP-bdc) and 2,5-bis(*n*-butoxy)benzenedicarboxylic acid (H_2BB-bdc). Analogous syntheses using H_2BMP-bdc and H_2BB-bdc with $Zn(NO_3)_2\cdot 6H_2O$ and bipy in DMF/EtOH yield MOF materials isostructural to **1**, as evidenced by PXRD and IR spectroscopy (Figures S13 and S14). However, using 2,5-substituted H_2bdc for Zn^{2+}-based MOFs without any coligand does not lead to new topologies by necessity. We studied the implementation of BME-bdc and some of the above-mentioned linkers L into the series of MOF-5 isotypes $[Zn_4OL_3]$.[8]

A sample of $\mathbf{1}_{as}$ was activated by soaking in $CHCl_3$ and drying at 140 °C *in vacuo* to achieve $\mathbf{1}_{dry}$. PXRD of $\mathbf{1}_{dry}$ shows that the structure is still intact after guest removal (Figure S3). Moreover, $\mathbf{1}_{dry}$ is insoluble and stable in common organic solvents (namely EtOH, THF, MeCN, hexane, acetone, toluene, DMSO), as shown by PXRD analyses (Figure S4). However, exposing $\mathbf{1}_{dry}$ to water vapor irreversibly transforms the structure to a so-far unknown crystalline phase (Figure S5). It is supposed that a MOF based on Zn−carboxylates cannot hold large amounts of moisture without structural decomposition, if it is not specifically functionalized to be very hydrophobic.[9]

dx.doi.org/10.1021/ja109317e |*J. Am. Chem. Soc.* 2011, 133, 2064–2067

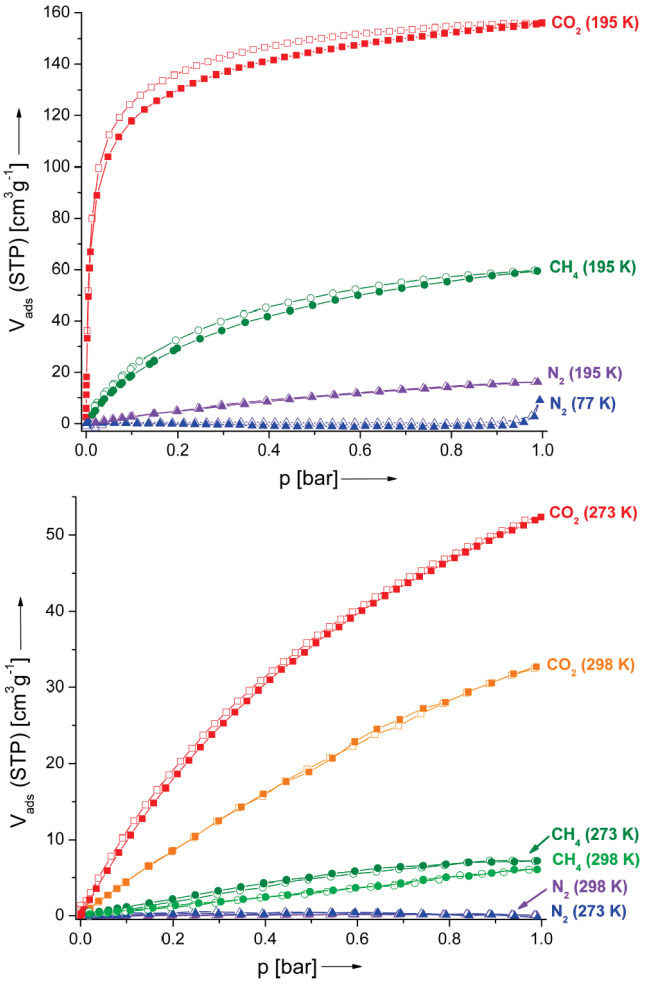

Figure 4. Sorption isotherms recorded on $\mathbf{1}_{dry}$. Adsorption and desorption branches are shown with closed and open symbols, respectively.

The material $\mathbf{1}_{dry}$ is expected to show selective sorption properties toward small polar molecules due to its polar, solvent-like $CH_3-O-C_2H_4$ chains.[8] In order to analyze the sorption behavior of $\mathbf{1}_{dry}$, N_2, CO_2, and CH_4 sorption isotherms were recorded at various temperatures (Figure 4). Interestingly, $\mathbf{1}_{dry}$ does not adsorb any nitrogen at 77 K. Raising the temperature to 195 K increases the sorption capacity only slightly. At 77 K, the methoxyethoxy chains have quite low thermal energy and lock the pore aperture windows, keeping out nitrogen molecules like a molecular gate. Raising the temperature to 195 K increases the thermal motion of the flexible chains, which makes it easier for N_2 to penetrate into the channels of $\mathbf{1}_{dry}$. Increasing the temperature further to 273 or 298 K decreases the N_2 sorption capacity again toward almost zero, as expected for thermodynamic reasons. Therefore, the adsorption at 273 and 298 K can be attributed to adsorption on the outer surface of the MOF powder and not in the porous structure.

The CO_2 sorption measurements at 195, 273, and 298 K show typical type I isotherms with high uptake (Table 1). At 195 K, a steep increase of the CO_2 uptake takes place in the low-pressure region (0.00−0.05 bar), and a small hysteresis is visible in the desorption branch. The hysteresis can be attributed to slow kinetics of adsorption. The uptake of CO_2 at 273 K and 1 bar is ∼500 times higher than the uptake of N_2 (∼10 times higher at 195 K; ∼300 times higher at 298 K) (Table 1). CH_4 sorption

Table 1. Adsorbed Volumes of N_2, CH_4, and CO_2 in $\mathbf{1}_{dry}$ at 1 bar

	V_{ads} ($cm^3\ g^{-1}$)		
T (K)	N_2	CH_4	CO_2
77	∼0.1	–	–
195	16	60	156
273	∼0.1	7	52
298	∼0.1	6	33

isotherms at 195, 273, and 298 K show higher uptakes than for N_2, but much less so compared to CO_2 at the same temperature.

The sorption of gas mixtures in porous materials can be reliably estimated from single-component sorption isotherms.[10] Therefore, we determined the initial slopes in the Henry region of the adsorption isotherms of $\mathbf{1}_{dry}$ (Figures S15−S17). The ratios of the slopes were used to estimate the sorption selectivities for CO_2 over N_2 and for CO_2 over CH_4. From these data, the CO_2/N_2 selectivity is 84:1 at 273 K (611:1 at 195 K and 40:1 at 298 K). To the best of our knowledge, this selectivity is slightly higher than the highest selectivity reported previously at this temperature.[11] The CO_2/CH_4 selectivity is 9:1 at 273 K (77:1 at 195 K and 9:1 at 298 K). The sorption selectivity of $\mathbf{1}_{dry}$ is not due to a simple size-sieving effect. CH_4 is bigger than N_2, but it has a higher polarizability and may interact more strongly with the polar pore surface of $\mathbf{1}_{dry}$. Therefore, increased adsorption is expected. These data indicate that $\mathbf{1}_{dry}$ can compete with the benchmark MOFs for highly selective CO_2 capture.[11,12] This substantiates the concept of using alkyl ether side chains. The flexibility of these substituents will have a major effect on the performance of $\mathbf{1}_{dry}$ in the adsorption of multicomponent gas mixtures. Therefore, breakthrough measurements as well as multicomponent adsorption measurements are a matter of ongoing work in our laboratories. However, the reactivity of $\mathbf{1}_{dry}$ toward water suggests that the material will not have real-life application in CO_2 capture. Using other metal centers instead of Zn^{2+}, e.g., Mg^{2+} and Co^{2+}, exhibiting a suitable coordination chemistry, isoreticular congeners of **1** may be accessible, which are likely to be much more water tolerant and may therefore be of potential interest for CO_2 capture under industrial conditions.

In conclusion, we have demonstrated a novel concept of using tailored linker functionalization to trigger otherwise inaccessible MOF network topologies for an important MOF family of highly variable $[M_2L_2P]_n$ compositions. The particular alkyl ether substituents do not interfere with the MOF synthesis (e.g., avoiding open-framework formation) but rather have a major impact on the conformational freedom of the carboxylate groups of the linker, which is the key for obtaining a previously unknown, functionalized honeycomb-like structure. The obtained MOF shows ultrahigh selective sorption of CO_2 over N_2 and CH_4, suggesting possible applications in capturing CO_2 from flue gases or upgrading natural gas by CO_2/CH_4 separations, if water-tolerant isoreticular derivatives can be made. The concept is extendable to a series of isoreticular frameworks by employing other 2,5-disubstituted bdc derivatives. In principle, a wide variety of functional groups can be integrated to design the coordination space of the material for specific applications in gas adsorption and separation. Future work will examine how the sorption properties of the materials depend on the nature and the combinations of the substituents with particular respect to the concept of multivariate MOFs introduced by Yaghi and co-workers.[13]

dx.doi.org/10.1021/ja109317e |*J. Am. Chem. Soc.* 2011, 133, 2064–2067

■ ASSOCIATED CONTENT

Supporting Information. Detailed synthesis procedures, CIF files of $\mathbf{1}_{as}$ and **2**, and further analytical data (Figures S1−S17). This material is available free of charge via the Internet at http://pubs.acs.org.

■ AUTHOR INFORMATION

Corresponding Author
roland.fischer@ruhr-uni-bochum.de

■ ACKNOWLEDGMENT

The authors gratefully thank Prof. C. W. Lehmann and A. Dreier from the Max-Planck Institute für Kohlenforschung (Mühlheim an der Ruhr, Germany) for collecting single-crystal X-ray diffraction data of $\mathbf{1}_{as}$. The Priority Program 1362 of the German Research Foundation on "Metal-Organic Frameworks" is acknowledged for funding. The Research School of the Ruhr-Universität Bochum and the Fonds der chemischen Industrie are acknowledged for fellowships (S.H.).

■ REFERENCES

(1) (a) Eddaoudi, M.; Kim, J.; Rosi, N.; Vodak, D.; Wachter, J.; O'Keeffe, M.; Yaghi, O. M. *Science* **2002**, *295*, 469–472. (b) Millward, A. R.; Yaghi, O. M. *J. Am. Chem. Soc.* **2005**, *127*, 17998–17999. (c) Dinca, M.; Long, J. *Angew. Chem., Int. Ed.* **2008**, *47*, 6766–6779.

(2) (a) Lee, J. Y.; Farha, O. K.; Roberts, J.; Scheidt, K. A.; Nguyen, S. T.; Hupp, J. T. *Chem. Soc. Rev.* **2009**, *38*, 1450–1459. (b) Farrusseng, D.; Aguado, S.; Pinel, C. *Angew. Chem., Int. Ed.* **2009**, *48*, 7502–7513.

(3) (a) Li, J.-R.; Kuppler, R. J.; Zhou, H.-C. *Chem. Soc. Rev.* **2009**, *38*, 1477–1504. (b) Chen, B.; Xiang, S.; Qian, G. *Acc. Chem. Res.* **2010**, *43*, 1115–1124. (c) Zhang, J.-P.; Chen, X.-M. *J. Am. Chem. Soc.* **2008**, *130*, 6010–6017.

(4) (a) Furukawa, H.; Kim, J.; Ockwig, N. W.; O'Keeffe, M.; Yaghi, O. M. *J. Am. Chem. Soc.* **2008**, *130*, 11650–11661. (b) Eddaoudi, M.; Kim, J.; O'Keeffe, M.; Yaghi, O. M. *J. Am. Chem. Soc.* **2002**, *123*, 376–377. (c) Eddaoudi, M.; Kim, J.; Vodak, D.; Sudik, A.; Wachter, J.; O'Keeffe, M.; Yaghi, O. M. *Proc. Natl. Acad. Sci. U.S.A.* **2002**, *99*, 4900–4904.

(5) See for example: (a) Dybtsev, D.; Chun, H.; Kim, K. *Angew. Chem., Int. Ed.* **2004**, *43*, 5033–5036. (b) Ma, B.-Q.; Mulfort, K. L.; Hupp, J. T. *Inorg. Chem.* **2005**, *44*, 4912–4914. (c) Chen, B.; Liang, C.; Yang, J.; Contreras, D. S.; Clancy, Y. L.; Lobkovsky, E. B.; Yaghi, O. M.; Dai, S. *Angew. Chem., Int. Ed.* **2006**, *45*, 1390–1393. (d) Chun, H.; Dybtsev, D. N.; Kim, H.; Kim, K. *Chem. Eur. J.* **2005**, *11*, 3521–3529. (e) Horike, S.; Matsuda, R.; Tanaka, D.; Matsubara, S.; Mizuno, M.; Endo, K.; Kitagawa, S. *Angew. Chem., Int. Ed.* **2006**, *45*, 7226–7230. (f) Chen, B.; Ma, S.; Hurtado, E. J.; Lobkovsky, E. B.; Zhou, H. C. *Inorg. Chem.* **2007**, *46*, 8490–8492.

(6) (a) Chun, H.; Moon, J. *Inorg. Chem.* **2007**, *46*, 4371–4373. (b) Frišić, T.; Reid, D. G.; Halasz, I.; Stein, R. S.; Dinnebier, R. E.; Duer, M. L. *Angew. Chem., Int. Ed.* **2010**, *49*, 712–715. (c) Kondo, M.; Takashima, Y.; Seo, J.; Kitagawa, S.; Furukawa, S. *Cryst. Eng. Commun.* **2010**, *12*, 2350–2353.

(7) (a) Singh, B.; Long, J. R.; Fabrizi de Biani, F.; Gatteschi, D.; Stavropoulos, P. *J. Am. Chem. Soc.* **1997**, *119*, 7030–7047. (b) Kumar, U.; Thomas, J.; Thirupathi, N. *Inorg. Chem.* **2010**, *49*, 62–72.

(8) Henke, S.; Schmid, R.; Grunwaldt, J.-D.; Fischer, R. A. *Chem. Eur. J.* **2010**, *48*, 14296–14306.

(9) (a) Greathouse, J. A.; Allendorf, M. D. *J. Am. Chem. Soc.* **2006**, *128*, 10678–10679. (b) Schröck, K.; Schröder, F.; Heyden, M.; Fischer, R. A.; Havenith, M. *Phys. Chem. Chem. Phys.* **2008**, *10*, 4732–4739. (c) Low, J. J.; Benin, A. I.; Jakubczak, P.; Abrahamian, J. F.; Faheem, S. A.; Willis, R. R. *J. Am. Chem. Soc.* **2009**, *131*, 15834–15842. (d) Nguyen, J. L.; Cohen, S. M. *J. Am. Chem. Soc.* **2010**, *132*, 4560–4561.

(10) (a) Myers, A. L.; Prausnitz, J. M. *AIChE J.* **1965**, *11*, 121–127. (b) Bae, Y.-S.; Farha, O. K.; Spokoyny, A. M.; Mirkin, C. A.; Hupp, J. T.; Snurr, R. Q. *Chem. Commun.* **2008**, 4135–4137. (c) Bae, Y.-S.; Farha, O. K.; Hupp, J. T.; Snurr, R. Q. *J. Mater. Chem.* **2009**, *19*, 2131–2134.

(11) An, J.; Geib, S. J.; Rosi, N. L. *J. Am. Chem. Soc.* **2010**, *132*, 38–39.

(12) (a) Banerjee, R.; Furukawa, H.; Britt, D.; Knobler, C.; O'Keeffe, M.; Yaghi, O. M. *J. Am. Chem. Soc.* **2009**, *131*, 3875–3877. (b) Demessence, A.; D'Alessandro, D. M.; Lin Foo, M.; Long, J. R. *J. Am. Chem. Soc.* **2009**, *131*, 8784–8786. (c) Wang, B.; Côte, A. P.; Furukawa, H.; O'Keeffe, M.; Yaghi, O. M. *Nature* **2008**, *453*, 207–212. (d) Vaidhyanathan, R.; Iremonger, S. S.; Dawson, K. W.; Shimizu, G. K. H. *Chem. Commun.* **2009**, 5230–5232. (e) Choi, H.-S.; Suh, M. P. *Angew. Chem., Int. Ed.* **2009**, *48*, 6865–6869.

(13) Deng, H.; Doonan, J. Ch.; Furukawa, H.; Ferreira, R. B.; Towne, J.; Knobler, C. B.; Wang, B.; Yaghi, O. M. *Science* **2010**, *327*, 846–850.